Injury 50 (2019) 1612–1619

Contents lists available at ScienceDirect

Injury

journal homepage: www.elsevier.com/locate/injury

A novel adjustable locking plate (ALP) for segmental bone fracture treatment

Omer Subasi, Atacan Oral, Ismail Lazoglu*

Manufacturing and Automation Research Center, Koc University, Istanbul 34450, Turkey

ARTICLE INFO

Article history:
Received 8 March 2019
Accepted 19 August 2019

Keywords:
Bone fracture
Bone plate
Adjustable dynamic plate
Locking compression plate
Finite element analysis
Bending strength
Fatigue life

ABSTRACT

A novel Ti6Al4V adjustable locking plate (ALP) is designed to provide enhanced bone stability for segmental bone fractures and to allow precise positioning of disconnected segments. The design incorporates an adjustable rack and pinion mechanism to perform compression, distraction and segment transfer during plate fixation surgery. The aim of this study is to introduce the advantages of the added feature and computationally characterize the biomechanical performance of the proposed design. Structural strength of the novel plate is analyzed using numerical methods for 4-point bending and fatigue properties, following ASTM standards. An additional mechanical failure finite element test is also conducted on the rack and pinion to reveal how much torque can be safely applied to the mechanism by the surgeon. Simulation results predict that the new design is sufficiently strong to not fail under regular anatomical loading scenarios with close bending strength and fatigue life properties to clinically used locking compression plates. The novel ALP design is expected to be a good candidate for addressing problems regarding fixation of multi-fragmentary bone fractures.

Introduction

Stabilization of fractures with compression plates are among the most widely used surgical treatments in orthopedics. While, in the past, dynamic compression plates (DCP) have been extensively used to provide absolute stability to the fracture site and promote fast primary healing, nowadays, the locking compression plates (LCP) have mostly replaced them [1,2]. By bridging the two ends of the fracture, LCPs provide relative stability to the site which promotes a slower but stronger secondary healing [2,3]. Relative stability also allows micromotions between the two ends of the fracture that helps callus formation at the early stages of healing [4]. Most commonly, LCPs are successfully utilized for treatment of upper extremity fractures [5–8].

The design behind the surgical fixation plates are straightforward, yet, rudimentary from an engineering point of view. Although LCPs have a gamut of advantages over its predecessor plate types, they are still static in nature and fail to properly address more complex complications such as multi-fragmented or comminuted fractures. Moreover, during the surgical operation, they allow no flexibility in terms of adjusting the geometry of the fracture; after the placement of the screws and locking of the plate, the fracture area is firmly stabilized. If there is a complication in the initial implementation of the plate that might lead to nonunion or malunion due to non-adequate support, there are no quick methods to modify to fracture line besides completely repositioning the plate [9]. Extra procedures during operations that lead to increased surgery duration, inevitably exacerbate the risk of infection and side effects of prolonged use of anesthesia on the patient [10].

In order to tackle the problems that arise from the inherent immobile design of straight plates, various adjustable plate designs have been proposed. This innovative research area in orthopedics also attempts to push the boundary of fracture fixation design to investigate potential benefits of having moving elements and added features to the simpler benchmark designs that could facilitate both the surgical procedures and enhance healing. However, adjustable plate studies are very limited in number and relatively recent in literature. Most notably, in 2016 Karakasli et al. proposed an adjustable design with an embedded spring mechanism that can generate compression forces up to 300 N [11]. Conducting in-vitro torsion and bending tests on 4th generation composite femurs, they have demonstrated that while the biomechanical performance was not compromised in comparison to a benchmark plate, the increased compressive forces at the fracture ends could facilitate bone healing [11].

Our research group proposed a novel, Ti6Al4V ALP design with an embedded rack and pinion mechanism, under WIPO, US

* Corresponding author.
E-mail address: ilazoglu@ku.edu.tr (I. Lazoglu).

https://doi.org/10.1016/j.injury.2019.08.034
0020-1383/

and EU patents (Patent numbers: WO2014033088A1, US9138270B2, EP2890313B1), that can perform different actions including, extension, distraction and segment transfer [12]. The plate is aimed to provide more options and flexibility to the surgeon for fracture line adjustment during operation. Furthermore, the advantages of this design for addressing multi-fragmentary fractures and bone extension and shortening operations are discussed in detail. The structural properties of the new design are predicted using numerical simulations to validate its biomechanical performance.

Plate design

The newly designed ALP is comprised of two main parts: the plate and the rack-pinion mechanism (Fig. 1). The plate portion is identical to a simple LCP with threaded screw holes. The only difference is that from the midpoint of the plate to one end, a small conduit exists such that the moving rack-pinion mechanism can be housed. An additional small hole, at the midpoint of the plate's top surface, allows the mounting of the pinion for external application of rotation. The rotation of the pinion is coupled with the rack member for conversion of rotating motion to linear displacement. The rack is the only sliding portion of the design and is specially designed with holes such that surgical screws can be implemented in regular fashion during plate fixation. The rest of the plate contains regular threaded holes for implementation of locking surgical screws.

The pinion can be easily rotated intraoperatively with an appropriate screwdriver or surgical fastener. The design incorporates a smaller hole near the pinion hole on top for locking of the pinion gear in place with a small locking pin, inserted between the teeth of the pinion, after the bone adjustment is completed. Consequently, the displacement of the sliding rack is restricted with this pin to avoid undesired knock-back response after the fracture ends are spatially adjusted. The geometry of the conduit housing further limits the sliding rack's range of motion. Although the ALP contains extra features, the flexibility of the proposed design comes from the fact that it can be simply used as LCPs by preemptively locking the rack-pinion mechanism.

Segment transfer

Having the capacity to carry out bone segment transfer in a fracture gap created between two ends of a long bone is critical for various reasons. For treatment of segmental defects in bone, the defected or infected portion of the bone can be osteotomized and replaced with healthier tissue via vascularized bone graft techniques [13]. However, such operations typically require nail guides that pass through the intermedullary canal along the bone length for axially precise positioning of the bone graft segment [14]. Any operation that includes placement of inserts are surgically more complicated in nature and due to increased contact area of bone with foreign material, the chance of infection is higher. With the novel ALP design, segment positioning can be accomplished without guide inserts as the plate will allow both fixation of fracture and segment positioning, simultaneously.

In addition, segment transfer is relevant for addressing segmental fracture fixation problems in long bones, in which more than one fracture line isolate and disconnect a portion of diaphysis from the ends. These cases carry a high risk of delayed union or malunion, such that the preservation of original bone anatomy must be handled with extra care and precision during fixation [15]. With simple LCPs, it is not possible to have any flexibility in correctly positioning the disconnected bone segment, but with the proposed ALP, the surgeon can separately handle and position the segment with respect to the ends to conserve long bone geometry and regulate the compression.

Fig. 2 shows the steps of the bone segment transfer operation that can be conducted with the ALP. The surgeon initially decides on the distance between the two ends of the long bone, between which the disconnected segment will be positioned. Using the static threaded holes on each end, the surgeon stabilizes the gap. The disconnected bone segment is, then, separately fixed to the holes on the sliding rack. Using the pinion, the segment is appropriately positioned in the bone gap; extra compression against the diaphysis can also be created by having the segment lean on one of the gap boundaries. The motion of the rack is then blocked with the insertion of the pinion lock, that keeps the bone segment in place.

Compression and distraction

Clinically utilized LCPs are designed for stabilizing the fracture area, but they do not provide any flexible means of fracture line adjustment. LCPs are successful when used as simple bridge fixators that provide relative stability to the fracture area to promote secondary healing pathways [3]. On the other hand, DCPs enable the surgeon to apply dynamic compression force between the two transfixed segments by pushing the round head of the surgical screw against the inclined screw hole to achieve absolute stability of the fracture [1,17]. Tension devices are also used during fixation to artificially create extra compression, but inevitably render the operation clunkier with added equipment and steps [16]. While DCPs offer fracture line adjustment to a certain extent, the manipulation method of pushing a screw against the slanted hole is not entirely flexible. Thus, our design incorporates the advantages of

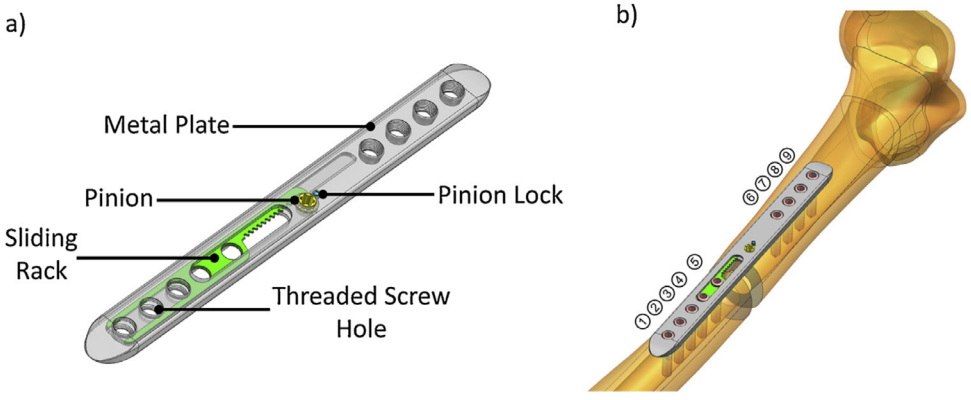

Fig. 1. (a) CAD model of the proposed ALP with the rack and pinion mechanism. The metal plate is illustrated with translucence to reveal the embedded mechanism inside the conduit. (b) CAD model of ALP fixed with threaded unicortical surgical screws (numbered 1 through 9) to stabilize a transverse diaphyseal bone fracture.

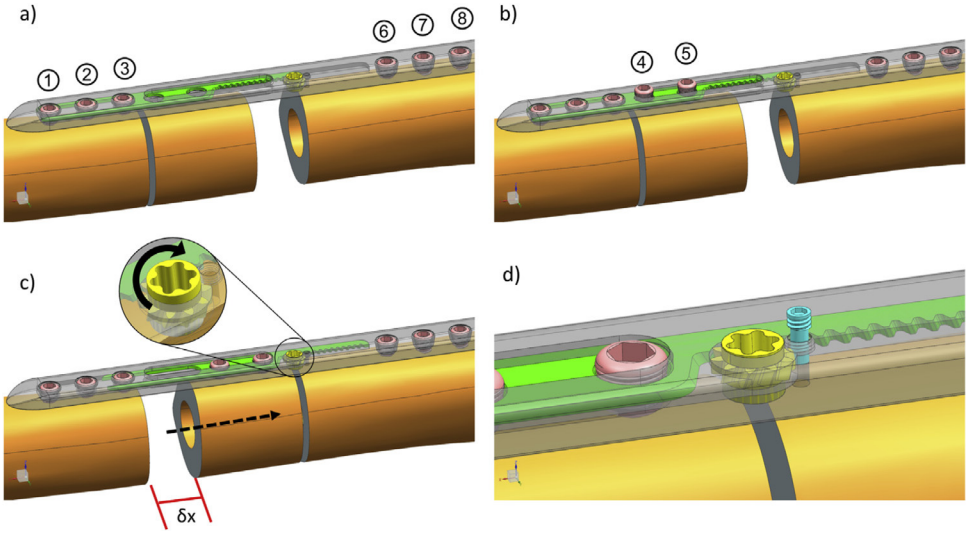

Fig. 2. Segment transfer operation with ALP. (a) The surgeon fixes the two ends of the bone using the stationary holes (1–3 & 6–9) at the opposite ends of the plate. (b) The disconnected segment is separately fixed using the holes (4 & 5) on the sliding rack. (c) By rotating the pinion, segment positioning, compression or distraction is achieved. (d) The locking pin is inserted after transfer completion to restrict the mechanism's motion.

both designs, in which locking screws with superior plate-screw coupling are used along with a compression mechanism similar in nature to DCP, but with a more controlled and precise manipulation method.

The ALP design is also aimed to facilitate and provide another alternative to bone shortening and extension surgeries. Bone shortening operations are straightforward with the fixation plates already in use, but design of orthopedic devices to conduct bone lengthening is still a topic of research. External fixators such as Ilzarov and monoplanar fixtures have been utilized in the past, but today intermedullary nailing is widely used for this operation [18]. Due to the long healing periods of the bone, external fixators cause discomfort for the patient [18]. Intermedullary nails are used to high success today, yet the increased contact area between the implant and the bone tissue leads to higher risks of infection and nerve damage [19]. The novel ALP can be used as an LCP with limited the contact to the bone, bypassing a potential downside of intermedullary fixing.

Furthermore, the surgery related complications are much fewer compared to the other options. While conducting a bone extension surgery with an intermedullary nail, attachment of distal and proximal interlocking screws poses a great challenge. Typically, the screws are inserted using freehand technique with fluoroscopic guidance during surgery [28]. Other computer assisted methods for screw insertion guidance are also proposed in literature [29]. Yet, these techniques are not cost-effective options. Consequently, conducting such surgeries with the proposed ALP provides a much easier fixation since the plate holes are readily visible and accessible by the surgeon.

Fig. 3 demonstrates the stabilization of an oblique fracture with the ALP. The critical difference in steps is that, initially, one segment is fixed with stationary holes, while the opposing segment

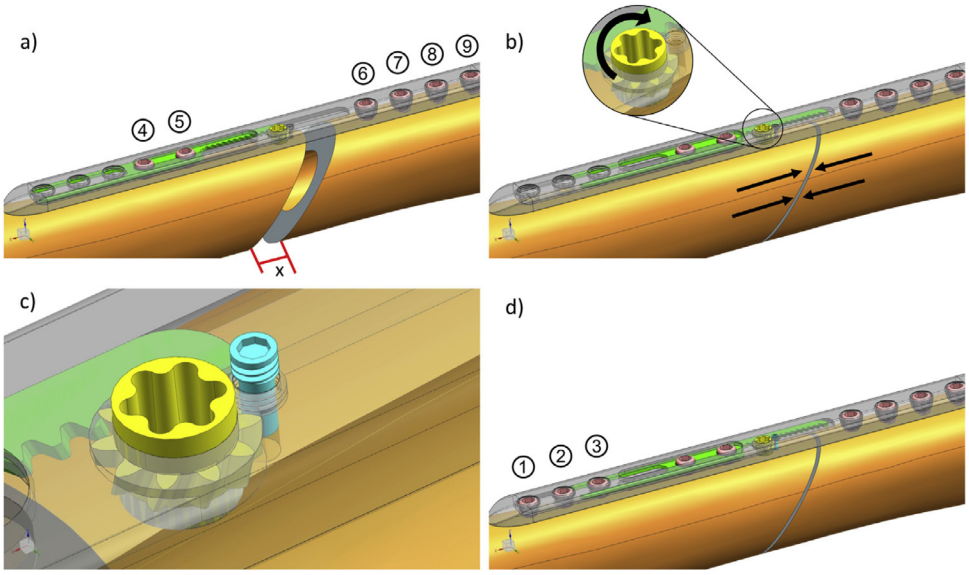

Fig. 3. Fracture stabilization and compression operation with ALP. (a) The surgeon fixes one end of the fractured bone with the stationary holes (6–9) but other end with only the sliding rack holes (4 & 5). (b) By rotating the pinion, one end of the fracture can be pressed against the other and the fracture line is manipulated. (c) The locking pin is inserted after compression to stop pinion's rotation. (d) The remaining stationary holes (1–3) are fixed to completely stabilize the fracture.

is fixed with only the holes on the moving rack. Thus, by rotating the pinion, the segment attached to the rack can be displaced relative to the stationary segment. Without the need of other tools, distraction, shortening and compression can be easily carried out. The mechanism is locked after and with the insertion of the screws to the remaining stationary holes, the facture is completely stabilized.

Materials and methods

Manufacturing

The ALP is manufactured from biocompatible Titanium alloy (Ti6Al4V), shown in Fig. 4. The important dimensional parameters of the plate are presented in Table 1. Since there is a conduit inside the metal plate, the main plate and the base cover of the conduit are manufactured separately and then welded together after the placement of the rack-pinion mechanism. The small pinion is produced separately with a 5-axis CNC milling center as it is not possible to machine the helical teeth profile in 3-axis. Polishing is carried out afterwards to reduce the surface roughness of the plate.

Preliminary mechanism test

A preliminary in-vitro test is conducted with a manufactured prototype of the ALP on a human femur model (SYNBONE, Graubunden, Switzerland) to examine the operability of the sliding mechanism during surgery (Fig. 5). The plate is first fixed to the bone from two stationary holes at each end of the ALP via guide drilling and insertion of screws. The sliding rack-pinion is checked after this initial fixation to confirm that the mechanism is operating as intended without obstruction. Using a saw blade, a mock transverse osteotomy is conducted to create a 2 cm gap in the diaphysis and an isolated bone segment of 5 cm, such that the isolated segment could be moved along the gap by rotating the pinion. After the segment is fixed to the moving hole on the sliding rack, the mechanism was successfully operated to conduct segment transfer.

Computational analysis

In comparison to simple internal fixators like LCP and DCP, which are straight plates with only screw holes, the ALP design introduces a conduit that runs along a portion of the plate that inevitably impacts the stiffness. Furthermore, there are dynamically interacting pieces introduced to the system, which create additional uncertainties and performance parameters. Two critical in-vitro biomechanical tests are 4-point bending (FPB) and fatigue tests as outlined by the ASTM F382-17 standards for metallic bone plates [21]. Thus, for the computational study, bending, and fatigue tests are done on ANSYS software, version 17.2. Table 2 contains the material properties of Ti6Al4V used for all the simulations.

Table 1
Dimensional parameters of ALP.

Length	175 mm
Width	15 mm
Thickness	4.2 mm
Range of sliding motion	35 mm
Bone surface crescent radius	90 mm

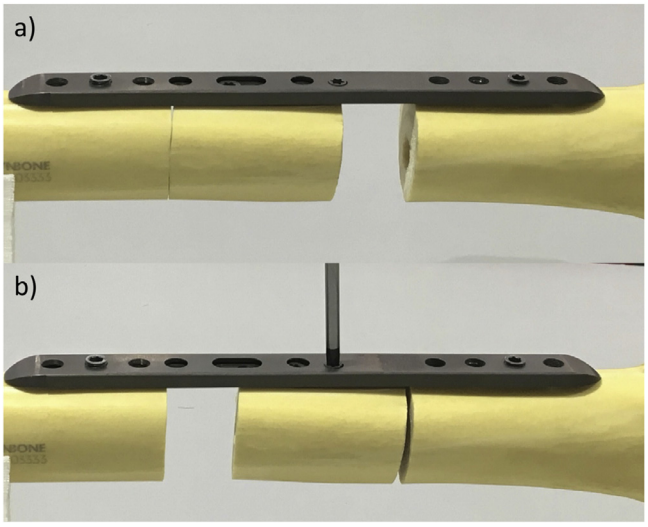

Fig. 5. Preliminary testing of ALP on a human femur model. A mock transverse osteotomy is conducted from two points to isolate a 5 cm bone segment and simulate a 2 cm gap. (a) The plate is secured to a composite femur with a screw on each end using the stationary holes and the isolated segment is fixed to the sliding rack. (b) The pinion is successfully operated to move the disconnected segment.

Table 2
Mechanical properties of Ti6Al4V used in FEA.

Density	4429 kg/m^3
Young's Modulus	113.8 GPa
Poisson's ratio	0.342
Yield Strength	790 MPa
Ultimate Tensile Strength	860 MPa
Tangent Modulus [24]	1250 MPa

It is possible to characterize the bending stiffness and strength by applying FPB conditions on the bone plate. Since a larger area is put under maximum stress compared to 3-point bending test, stress accumulation points can be more easily revealed, which is critical for asymmetric plate designs. Fig. 6 and Table 3 show the static structural FE test model and parameters, respectively. The loading pushers are designed similarly to rollers that match the crescent radius of the plate surface. The conduit, which creates the asymmetry in the geometry, is placed in between the pushers. Both the supports and pushers contact the plate at smooth surfaces that are not interrupted by screw holes. Also, hole threading has been removed on the plate holes to avoid the potential notching effect [27].

Fig. 4. Manufactured ALP and surgical locking screws.

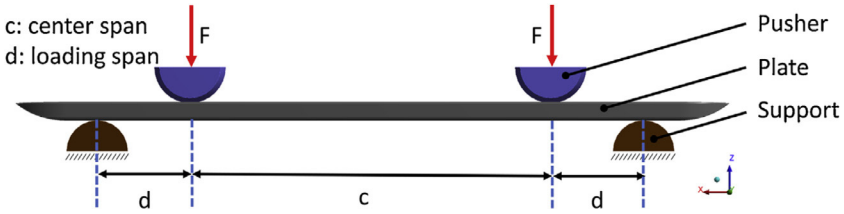

Fig. 6. CAD model of FPB finite element analysis setup. The conditions are replicated from ASTM standards.

Table 3
FE parameters for FPB.

Center span (c)	88.5 mm
Loading Span (d)	22.75 mm
Constraints	Fixed supports, pusher and plate constrained in X and Y direction
Loading	Incremental displacement control on pushers
Mesh	Tetrahedral elements with adaptive sizing
Element Number	71914
Node Number	114583

The FPB is conducted with displacement control on the pushers until the ultimate tensile strength point of the plate has been exceeded. Bilinear isotropic hardening using von Mises yield criteria has been assumed for the behavior of the material until ultimate tensile strength (UTS). The tangent modulus used to describe the plastic behavior of the material is obtained from a study [24].

In addition, an FE model identical to Fig. 6 is used to simulate the fatigue property with the same FE parameters. In addition, a reference S-N (stress-cycle) fatigue data for Ti6Al4V, obtained from a study, is assigned to the material [25]. To derive the characteristic moment-cycle curve for the plate, minimum fatigue life is obtained for twenty different alternating force values ranging from 3000 to 4000 N applied to the top of the pushers.

Lastly, the rack-pinion mechanism, as a moving element in the ALP, requires an additional strength analysis. The interaction between the rack and gear teeth set the limit for how much compression can be applied between two segments of the bone via adjusting the pinion. If the accumulated stress on the teeth exceed the elastic limit of the material, there will be plastic deformation on the teeth, or the mechanism will fail by tooth breakage. To alleviate the stress accumulation, the pinion and rack teeth are designed and manufactured with 20° helix angle. To simulate this, another static structural FEA is conducted on only the rack and the pinion engagement.

For this part of the study, the pinion failure FEA strategy employed by Cao and Zhang is adopted [26]. To simulate the rack and pinion engagement, only a single contacting pair of teeth is utilized in the FE model. Boundary condition set for the simulation is fixing the rack from the bottom and applying a moment of rotation to the pinion; displacements in Y and Z axes are also set to zero for both parts. This set of constraints simulates the operation of the mechanism by the surgeon via applying rotation on the pinion during the adjustment of compression.

Frictionless type contact pairing between the teeth surfaces is established with software-controlled stiffness coefficient through the simulation. Table 4 contains the pertaining FE parameters. Tetrahedral mesh elements with adaptive sizing have been used with added mesh refining on the contacting surfaces (Fig. 9a). Chosen mesh for the model has been investigated for mesh sensitivity to ensure the results do not change with a finer mesh size. Using the same plasticity model, moment of rotation on the pinion teeth has been increased until the UTS has been reached.

Table 4
Rack and pinion parameters and FEA statistics.

	Profile	Thickness	Gear Module	Elements	Nodes
Rack	Straight Line	1 mm	0.7	65270	96248
Pinion	Involute	1.5 mm		50004	73591

Results

Four point bending

Fig. 7a demonstrates the von Mises stress result at 1.8 mm displacement of the pushers, indicating that for the given bending force, the plate starts yielding and going under plastic irrecoverable deformation. At this point of the bending, at least a single region passes the UTS of the material, which signifies failure. Stress accumulation points around the center pinion hole and the conduit window can be easily observed. Max stress versus pusher displacement graph is obtained from the simulation (Fig. 7b), which follows a similar trend to the bilinear hardening curve defined for the material. The plate is assumed to fail at this pusher displacement, thus the force reaction obtained from the pushers up until this point defines the maximum bending strength (Fig. 7c).

Linear variable differential transformer sensors used in traditional mechanical testing instruments can provide the load data over the pusher displacement, which reveals an approximate overall bending strength of the plate. However, with FE methods, it is possible to realize the at which point failure starts by observing the stress map. While the load-displacement graph obtained from a testing instrument will follow a decreasing trend after the elastic region towards the complete failure of the plate, Fig. 7c demonstrates the forces only up to the point a single region passes the ultimate strength level. This is the reason the decreasing trend cannot be observed in Fig. 7c and the 0.2% offset displacement point is simply assumed to be this first breaking point for this study.

Force displacement relationship allows the calculation of the critical mechanical properties outlined by ASTM standards. By using the total force at the failure point ($F_{failure}$), bending strength of the ALP can be calculated using,

$$M_{max} = \frac{F_{failure}}{2} \; x \; d \tag{1}$$

in which, M_{max} denotes the maximum bending moment, calculated as 36.28 Nm. Bending stiffness, which is another critical bone plate parameter for stress shielding considerations is calculated by,

$$K = \max\left(\frac{\Delta \text{Force}}{\Delta \text{Displacement}}\right) \tag{2}$$

in which K, denotes the linear stiffness of the plate derived from the elastic region in bending test. Maximum slope in the elastic region is found as 1775 N/mm which signifies the bending stiffness of the ALP.

Fatigue

Fatigue analysis demonstrates the structural endurance of the plate under cyclic loading. The plate is expected to remain

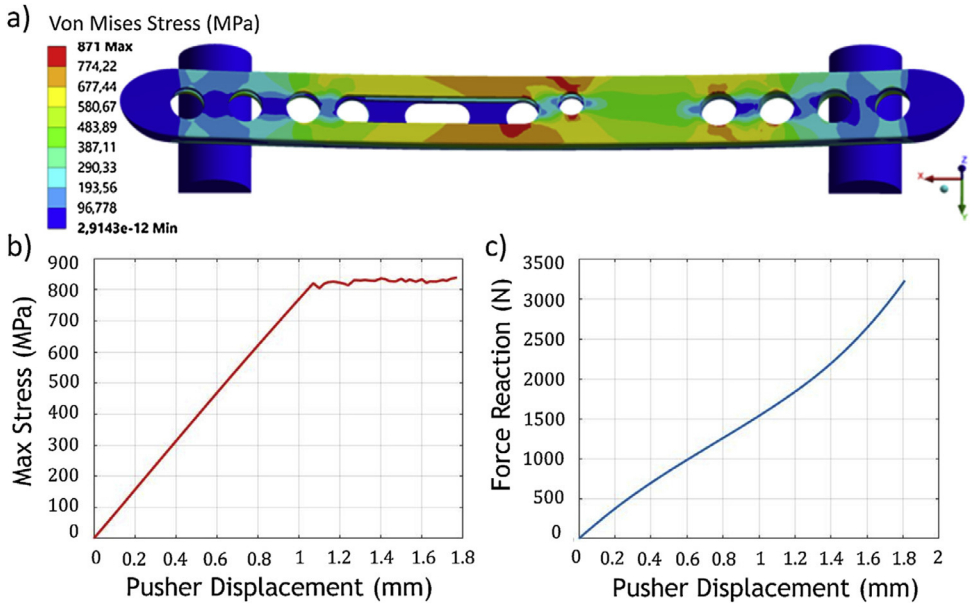

Fig. 7. (a) FEA stress results after yielding, near UTS. (b) Maximum stress and (c) total force reaction that occurs over pusher displacement.

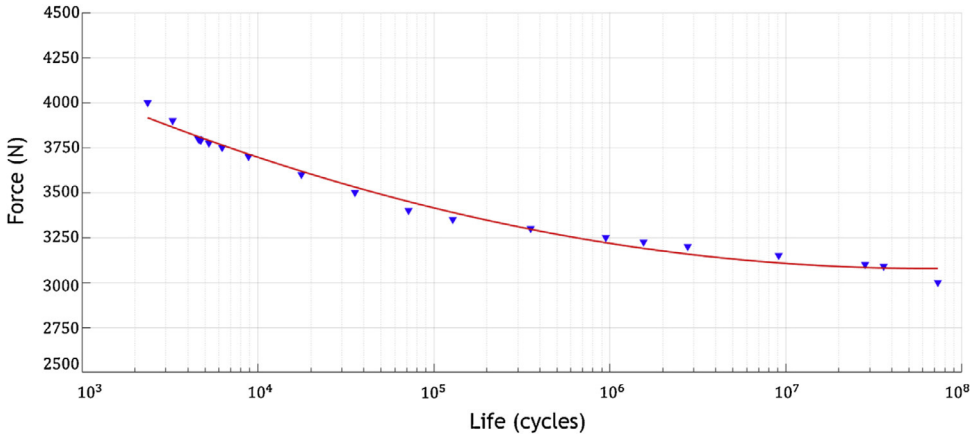

Fig. 8. Force-Cycle fatigue curve of ALP derived from FEA.

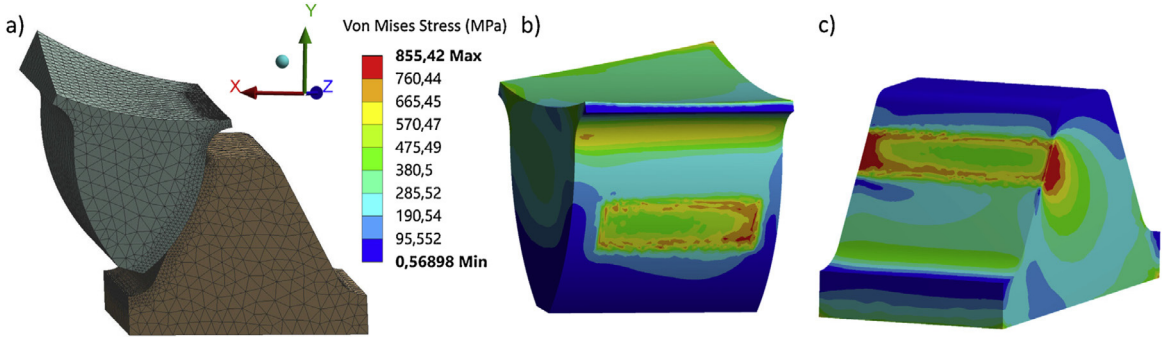

Fig. 9. (a) Meshing of teeth model. Max stresses on (b) pinion tooth and (c) rack tooth at failure.

implanted to the patient until complete recovery is achieved, which may reach 3 months for even a simple radial bone fracture. Over its lifetime, the plate must endure the repeating bending moment exerted on it caused by the daily physical activities of the patient, which renders its fatigue life an important design parameter. It is possible to derive a characteristic fatigue curve that represents how many cycles on average of a designated alternating stress will lead to the failure of the plate.

A characteristic Wohler curve is then obtained by creating a polynomial fit to the data points (Fig. 8). As expected, the fatigue life decreases as the loading on the ALP increases. At the bending moment caused by 3220 N alternating force, the minimum life

Table 5
Comparison of bending stiffness and fatigue life between the proposed ALP and the similar plates experimentally tested by Tsang et al.

	Analysis Type	Bending Stiffness (N/mm)	Fatigue life at alternating 2300 N (10^3 cycles)	Fatigue life at alternating 3500 N (10^3 cycles)
Tseng et al. [27]	In-vitro	1901 ± 115	$10^6 <$	71.5 ± 48.0
This study	In-silico	1775	$10^6 <$	48.7

is found as 10^6 cycles, which corresponds to the mean fatigue strength defined by the ASTM standards [21].

Rack-pinion strength

In Fig. 9a and b, as expected, the stress accumulation is in banded form on the contact surfaces and at the root regions. At 1700 Nmm moment applied on the pinion, stresses on the contact surface of the rack reach the UTS ceiling which suggests mechanism failure. Hence, the maximum torque that can be applied by the surgeon on the rack and pinion compression mechanism is limited to 1700 Nmm. The maximum contact and root stresses at the rack tooth are 855 and 469 MPa, respectively. The pinion tooth is exposed to 786 MPa at the contact and 675 MPa at the root region, again at the same moment loading scenario. The maximum strength identified for the rack and pinion is also relevant for cases in which the pinion is locked with the pin and the mechanism needs to endure the knock-back loads acting reciprocal to the compression. However, the plate is intended to be ultimately fixed using the stationary holes at the distal and proximal ends of the plate for all types of fracture gap stabilization, such that the sliding portion of the plate will never carry complete anatomical loads.

Discussion and conclusion

In this study, a novel bone plate design is proposed to address problems regarding fixation of segmental fractures while being able to also operate as a regular LCP. The in-vitro test, presented in Section 3.2, is only a preliminary assessment of the ALP to serve as a proof of concept for the design. However, the results of the demonstration were promising, indicating that no unseen complications should occur during the surgery and the surgeons would be able to intuitively operate the mechanism. The predetermined implementation steps demonstrated digitally in Section 2.1 and 2.2 are also validated.

To the best knowledge of the authors, characterization of ASTM outlined mechanical behavior of bone plates through finite element methods has not been discussed in literature. Typically, the performance of bone plates is either directly acquired through in-vitro experimentation [1,5,8,11,23,27] or bone model integrated FEA under anatomical loading scenario [3,20,22]. However, simulation of bending and fatigue tests on solely the bone plate with an integrated plasticity model after the yield point can help the prediction of mechanical behavior during the design stage of a novel plate with a more complex geometry. Especially, for plates deviating from a simple design with added features that render the manufacturing process complicated, like the proposed ALP, quick prediction of strength and stiffness via FE methods can be preferred over destructive performance tests to circumvent the production stage.

The necessity to resort to FE methods to obtain bending strength and fatigue life, parameters which are typically obtained directly via destructive experimentation, arose from the fact that the manufacturing of the complete plate assembly is labor-intensive, and an adequate number of plate specimens could not be manufactured at this point in time to obtain statistically significant experimental data. However, FE methodology followed in this study to directly obtain ASTM structural parameters could be critical in the future for quick analysis of designs that deviate from the simple plate designs, for which destructive testing might not be a feasible solution, especially at early design stages.

The results obtained from the simulations in Section 3.1 and 3.2 are validated by comparison to a similar study conducted by Tseng et al. [27]. In this study, notch sensitivity is investigated using straight, Titanium alloy, locking plates with 5 mm thickness, similar to our ALP geometry. The experimental data obtained by Tseng et al., also utilizing ASTM standards, is compared to the simulation results of the ALP in Table 5. Bending stiffness of the ALP is found to be slightly lower than the benchmark plate, which is expected due to the presence of the hollow conduit portion that houses the rack and pinion mechanism. Fatigue life results also share a similar trend.

The decreased bending strength is among the disadvantages of the proposed design. Even though lower stiffness could slightly alleviate stress shielding complications, under extreme loadings and impacts, the structurally weaker plate will yield and fail sooner. The large conduit openings of the plate, at the top and the bottom, are regions subjected to high stress accumulation, which could serve as premature crack initiation points as observed in Fig. 7a. Moreover, introducing moving elements brings a handful of mechanical uncertainties. Despite the fact that the design can function as a regular locking plate by preemptively locking the pinion, the sliding mechanism can fail due to over-exertion of torque on the pinion for more complex operations such as isolated segment positioning and fracture line adjustment. Teeth breakage could cause the failure and obstruct the surgeon from carrying out intended operations that depend on the sliding mechanism. Also, the ALP's complexity in production causes an inevitable trade-off between increased utility over the simple LCP and DCP against the increased manufacturing costs.

For future studies, a much more comprehensive comparative study for a more precise validation of the FE methodology is to be conducted. Additionally, bone integrated in-vitro biomechanical tests and in-vivo application, in which the healing of the specimens will be followed, are planned to be carried out. In terms of fracture fixation theory, the geometry of the designed plate does not dramatically deviate from the designs used clinically today, thus, we do not expect significantly worse results compared to other internal fixation devices such as commercial DCPs and LCPs. Yet, the addition of the sliding element to the design could render bone plates much more versatile fixation devices, capable of solving more complicated fracture scenarios.

Acknowledgement

This research was supported by Koc University Manufacturing and Automation Research Center.

References

[1] Ahern BJ, Showalter BL, Elliott DM, Richardson DW, Getman LM. In vitro biomechanical comparison of a 4.5mm narrow locking compression plate construct versus a 4.5mm limited contact dynamic compression plate construct for arthrodesis of the equine proximal interphalangeal joint. Vet Surg 2013;42:335–9. doi:10.1111/j.1532-950X.2013.01111.x.

[2] Azboy I, Demirtas A, Uçar BY, Bulut M, Alemdar C, Özkul E. Effectiveness of locking versus dynamic compression plates for diaphyseal forearm fractures. Orthopedics 2013;36:e917–22. doi:10.3928/01477447-20130624-23.
[3] Stoffel K, Dieter U, Stachowiak G, Gächter A, Kuster MS. Biomechanical testing of the LCP — how can stability in locked internal fixators be controlled? Injury 2003;34. doi:10.1016/j.injury.2003.09.021.
[4] Miller DL, Goswami T. A review of locking compression plate biomechanics and their advantages as internal fixators in fracture healing. Clin Biomech 2007;22:1049–62. doi:10.1016/j.clinbiomech.2007.08.004.
[5] Liu W, Yang L, Kong X, An L, Hong G, Guo Z, et al. Stiffness of the locking compression plate as an external fixator for treating distal tibial fractures: a biomechanics study. BMC Musculoskelet Disord 2017;18:1–6. doi:10.1186/s12891-016-1384-1.
[6] Kanakaris NK, Giannoudis PV. Locking plate systems and their inherent hitches. Injury 2010;41:1213–19. doi:10.1016/j.injury.2010.09.038.
[7] Calbiyik M, Ipek D. Use of different methods of intramedullary nailing for fixation of distal radius fractures: a retrospective analysis of clinical and radiological outcomes. Med Sci Monit 2018;24:377–86. doi:10.12659/MSM.908762.
[8] Jabran A, Peach C, Ren L. Biomechanical analysis of plate systems for proximal humerus fractures: a systematic literature review. Biomed Eng Online 2018;17:1–30. doi:10.1186/s12938-018-0479-3.
[9] Antuña SA, Barco R. Essential techniques in elbow surgery; 2016. doi:10.1007/978-3-319-31575-1.
[10] Rightmire E, Zurakowski D, Vrahas M. Acute infections after fracture repair: management with hardware in place. Clin Orthop Relat Res 2008;466:466–72. doi:10.1007/s11999-007-0053-y.
[11] Karakasli A, Acar N, Karaarslan A, Ertem F, Havitcioglu H. A novel adjustable dynamic plate for treatment of long bone fractures: an in vitro biomechanical study. J Clin Orthop Trauma 2016;7:177–83. doi:10.1016/j.jcot.2016.08.006.
[12] Lazoglu I, et al. "US9138270B2- Bone Plate." Google Patents, Google, patents.google.com/patent/US9138270B2/zh-TW.
[13] Minami A, et al. Treatment of infected segmental defect of long bone with vascularized bone transfer. J Reconstr Microsurg 1992;8:75–82.
[14] Sparks DS, Wagels M, Taylor GI. Bone reconstruction: a history of vascularized bone transfer. Microsurgery 2018;38:7–13. doi:10.1002/micr.30260.
[15] Kostenuik P, Mirza FM. Fracture healing physiology and the quest for therapies for delayed healing and nonunion. J Orthop Res 2017;35:213–23. doi:10.1002/jor.23460.
[16] Wittner Bernd, Holz Ulrich, et al. In: Buckley Richard E, editor "Plates." AO principles of fracture management. THIEME; 2018. p. 169–84.
[17] Xiong Y, Zhao YF, Xing SX, Sun HZ, Du QY, Wang ZM, et al. Comparison of interface contact profiles of a new minimum contact locking compression plate and the limited contact dynamic compression plate. Int Orthop 2010;34:715–18. doi:10.1007/s00264-009-0836-8.
[18] Sailhan F. Bone lengthening (distraction osteogenesis): a literature review. Osteoporos Int 2011;22:2011–15. doi:10.1007/s00198-011-1613-2.
[19] Eveleigh RJ. A review of biomechanical studies of intramedullary nails. Med Eng Phys 1995;17:323–31. doi:10.1016/1350-4533(95)97311-C.
[20] Zhang W, Li J, Zhang H, Wang M, Li L, Zhou J, et al. Biomechanical assessment of single LISS versus double-plate osteosynthesis in the AO type 33-C2 fractures: a finite element analysis. Injury 2018;49:2142–6. doi:10.1016/j.injury.2018.10.011.
[21] F382-17 ASTM. Standart specification and test method for metallic bone plates. West Conshohocken, PA: ASTM International; 2017 www.astm.org.
[22] Zhou JJ, Zhao M, Liu D, Liu HY, Du CF. Biomechanical property of a newly designed assembly locking compression plate: three-dimensional finite element analysis. J Healthc Eng 2017:1–11 2017. doi:10.1155/2017/8590251.
[23] Ang BFH, Chen JY, Yew AKS, Chua SK, Chou SM, Chia SL, et al. Externalised locking compression plate as an alternative to the unilateral external fixator: a biomechanical comparative study of axial and torsional stiffness. Bone Joint Res 2017;6:216–23. doi:10.1302/2046-3758.64.2000470.
[24] Ziaja W. Finite element modelling of the fracture behaviour of surface treated Ti-6Al-4V alloy. Comput Mater Sci Surf Eng 2009;1:53–60.
[25] Janeček M, Nový F, Harcuba P, Stráský J, Trško L, Mhaede M, et al. The very high cycle fatigue behaviour of Ti-6Al-4V alloy. Acta Phys Pol A 2015;128:497–502. doi:10.12693/APhysPolA.128.497.
[26] Cao YG, Zhang SH. Failure analysis of a pinion of the jacking system of a jack-up platform. Eng Fail Anal 2013;33:212–21. doi:10.1016/j.engfailanal.2013.05.018.
[27] Tseng WJ, Chao CK, Wang CC, Lin J. Notch sensitivity jeopardizes titanium locking plate fatigue strength. Injury 2016;47:2726–32. doi:10.1016/j.injury.2016.09.036.
[28] Zelle BA, Boni G. Safe surgical technique: intramedullary nail fixation of tibial shaft fractures. Patient Saf Surg 2015;9. doi:10.1186/s13037-015-0086-1.
[29] Langfitt MK, Halvorson JJ, Scott AT, Smith BP, Russell GB, Jinnah RH, et al. Distal locking using an electromagnetic field-guided computer-based real-time system for orthopaedic trauma patients. J Orthop Trauma 2013;27:367–72. doi:10.1097/BOT.0b013e31828c2ad1.